

An AI-Ready Fine-Tuning Framework for Accurate Machine-Learning Interatomic Potentials in Solid–Solid Battery Interfaces

Xiaoqing Liu,^{†,‡} Xinyu Yu,^{¶,§} Yangshuai Wang,^{||} Zhe-Tao Sun,^{¶,§} Zedong Luo,[‡] Kehan Zeng,[‡] Teng Zhao,^{*,⊥,‡,#} Shou-Hang Bo,^{*,¶,}@} and Zhenli Xu^{*,†}

[†]*School of Mathematical Sciences, MOE-LSC and CMA-Shanghai, Shanghai Jiao Tong University, Shanghai 200240, China*

[‡]*Shanghai Jiao Tong University–Chongqing Institute of Artificial Intelligence, Chongqing 401329, China*

[¶]*Future Battery Research Center, Global Institute of Future Technology, Shanghai Jiao Tong University, Shanghai 200240, China*

[§]*Global College, Shanghai Jiao Tong University, Shanghai 200240, China*

^{||}*Department of Mathematics, National University of Singapore, 10 Lower Kent Ridge Road, Singapore*

[⊥]*Institute of Natural Sciences, Shanghai Jiao Tong University, Shanghai 200240, China*
[#]*SOG AI-Technology Co. Ltd., Shanghai 200240, China*

[@]*State Key Laboratory of Synergistic Chem-Bio Synthesis, School of Chemistry and Chemical Engineering, Shanghai Jiao Tong University, Shanghai 200240, China*

E-mail: zhaoteng_sjtu@sjtu.edu.cn; shouhang.bo@sjtu.edu.cn; xuzl@sjtu.edu.cn

¹X. Liu, X. Yu and Y. Wang contribute equally to this work.

²Corresponding authors: T. Zhao, S.-H. Bo and Z. Xu.

Abstract

Atomistic modeling of solid-solid battery interfaces is essential for understanding electro-chemo-mechanical coupling, but the complex interfacial chemistry and heterogeneous environments pose major challenges for quantum-accurate, data-efficient modeling. Herein, we propose an approach of fine-tuning with integrated replay and efficiency (FIRE), a general framework for universal machine-learning interatomic potentials by combining efficient configurational sampling with a replay-argumented continual strategy, achieving quantum-level accuracy at moderate cost. Across six solid-solid battery interface systems, FIRE consistently achieves root-mean-square errors in energy below 1 meV/atom and in force near 20 meV/Å, marking an order-of-magnitude improvement over existing models while requiring only 10% of the original datasets. In addition, the fine-tuned model successfully reproduces key mechanical and electrochemical properties of the materials, in close agreement with experimental data. The FIRE offers a generalizable and data-efficient approach for developing accurate interatomic potentials across diverse materials, enabling predictive simulations beyond the reach of first-principles methods.

Introduction

Solid-solid interfaces play a central role in governing the electro-chemo-mechanical behavior of battery materials, especially for solid-state batteries.^{1–3} However, different from solid-liquid interfaces in conventional batteries, the intrinsic complexity of solid-solid interfaces poses formidable challenges for atomistic modeling, which mainly lies in the following aspects. First, the configuration diversity of solid-solid interfaces that arises from defects and dislocations significantly increases the difficulty of data sampling. Second, the complexity of the structure and atomic environment makes traditional theoretical frameworks insufficient. Notably, solid-solid interfaces in batteries are often composed of multiple crystalline phases, resulting in complex phenomena such as interface mismatch. The existence of heterogeneous

chemical bonds requires a higher generalization ability for a theoretical model in the chemical space. Finally, multi-physics coupling, i.e. electro-chemo-mechanical coupling at solid-solid interfaces makes it impossible for single-scale research to fully understand the behavior of complex interfaces.⁴

Recent advances in machine-learning interatomic potentials (MLIPs)⁵⁻¹⁵ have opened the door to quantum-accurate simulations at scales far beyond the reach of first-principles methods. However, constructing robust MLIPs via from-scratch training remains highly data-intensive, often demanding a huge number of costly quantum calculations. This bottleneck is particularly severe for interfaces, where structural diversity and complex interactions generate vast configurational landscapes. On the other hand, beneficial from the development of large language model techniques and material database such as Materials Project,¹⁶ universal machine learning interatomic potentials (U-MLIPs) have emerged as general-purpose force fields, e.g., MACE-MP-0,¹⁷ CHGNet,¹⁸ EquiformerV2,¹⁹ MatterSim,²⁰ and DPA,²¹ among others.²²⁻²⁶ By the pretraining on chemically diverse datasets, these models are capable of capturing a wide range of atomic interactions while exhibiting strong generalization across material classes. To date, MLIPs or U-MLIPs have been explored in battery materials,²⁷⁻³⁷ receiving increasing attention as a promising paradigm for scalable and transferable atomistic modeling for battery materials and interfaces. However, the broad generality of U-MLIPs often comes at the cost of reduced accuracy for task-specific materials, limiting their ability to resolve the intricate electro-chemo-mechanical mechanisms governed by battery interfaces. Therefore, designing an efficient pipeline from data generation, sampling and training for U-MLIPs is crucial to achieving quantum accuracy for interfacial modeling of battery materials.

Here, we propose an approach of Fine-tuning with Integrated Replay and Efficiency (FIRE), a data-efficient fine-tuning framework for constructing accurate machine-learning force fields in solid-solid interfaces in battery systems. Task-specific fine-tuning³⁸ is an efficient approach to overcome the limitations of U-MLIPs mentioned above. However, efficient

configurational sampling is often difficult for systems of solid-solid interfaces. We develop a pre-fine-tuned model to generate a candidate configuration pool, so that the dimensionality reduction and clustering can be employed to prepare a refined dataset for the task-specific fine-tuning. On the other hand, for each epoch during the fine-tuning process, we subsample from pre-trained dataset (i.e., replay), and feed into the model together with refined dataset to suppress over-fitting and improve the accuracy. The resulting models achieve high-quality numerical performance and reliably reproduce key mechanical and electrochemical properties in close agreement with experimental measurements. The FIRE is broadly applicable to systems beyond batteries, facilitating solutions to data scarcity and enhancing understanding of multiphysics coupling behaviors at interfaces.

Results and Discussion

The schematic diagram on the key components of FIRE is illustrated in Figure 1. These components are designed to build accurate MLIPs with significantly reduced computational cost. As shown in Fig. 1 (A), we adopt a task-specific fine-tuning paradigm instead of the from-scratch training, so that the expressive architecture of a universal foundation model is retained with task-relevant parameters being updated selectively. This strategy preserves transferability and inductive biases inherited from large-scale pretraining, and significantly lowers data and training time requirements. To further enhance generalization and robustness, we develop a replay-augmented continual fine-tuning scheme (shown in Fig. 1 (B)). This approach interleaves training on a stream of task-specific datasets with periodic replay of pretraining samples, thereby mitigating catastrophic forgetting. Compared to naive full-parameter fine-tuning,³⁹ this method enables progressive adaptation to complex interfacial systems while maintaining the general knowledge encoded in the foundation model. This is especially beneficial for achieving stable and accurate molecular dynamics simulations in complex systems.

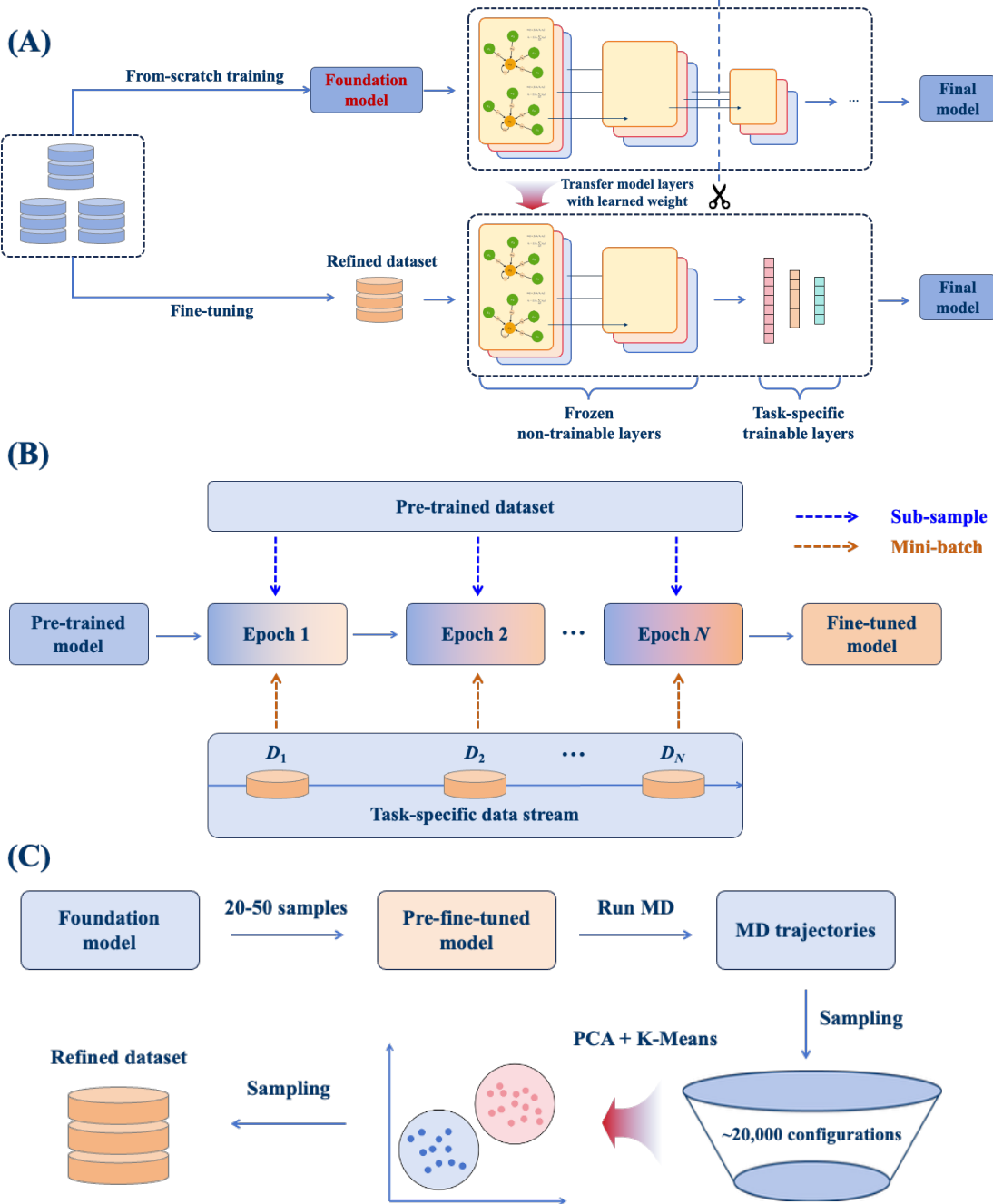


Figure 1: Overview of the FIRE framework: (A) comparison between from-scratch training and fine-tuning paradigms; (B) replay-augmented continual fine-tuning strategy that leverages both pretraining and task-specific datasets; (C) efficient sampling workflow, including a pre-fine-tuned model for robust MD generation, dimensionality reduction, and diversity-based selection of representative configurations.

In order to construct high-quality training datasets, we design an efficient and modular sampling protocol which is illustrated in Fig. 1 (C). The protocol begins with a pre-fine-tuned model trained on just 20–50 perturbed configurations, followed by molecular dynamics (MD) simulations to generate diverse atomic trajectories under realistic dynamics. This strategy significantly improves the stability and reliability of MD simulations, especially for complex systems requiring high-accuracy force fields. From the generated \sim 20,000 configurations, we select representative samples via PCA-assisted dimensionality reduction and K-means clustering on SOAP descriptors,^{40,41} yielding a compact yet informative training set. This process not only improves data efficiency but also ensures broad structural coverage, providing an AI-ready dataset for model fine-tuning.⁴² Full details on data preparation, including the generation of fine-tuning data from first-principles calculations and the fine-tuning protocols, are provided in Sections S.1 and S.2 of the *Supplementary Information* (SI).

To evaluate FIRE, we select six typical solid-solid interfaces in batteries that capture chemical and structural complexity of practical systems. These include electrode–electrolyte ($\text{Na}/\text{Na}_3\text{SbS}_4$, $\text{Li}/\text{Li}_6\text{PS}_5\text{Cl}$),^{43,44} coating in composite cathodes ($\text{Li}_3\text{PS}_4/\text{Li}_3\text{B}_{11}\text{O}_{18}$),⁴⁵ and solid electrolyte interphase at anodes ($\text{Li}_2\text{CO}_3/\text{LiF}$)⁴⁶ interfaces, as well as (electro)chemically disordered solid electrolyte ($\text{Li}_7\text{La}_3\text{Zr}_{2-x}\text{M}_x\text{O}_{12}$ ($M = \text{Ta}, \text{Nb}$), LiCl/GaF_3).^{47,48} The systems considered in this work capture key interfacial behaviors in solid-state batteries, providing a representative benchmark for evaluating the fine-tuning strategies. The snapshots of atomic configurations of these materials are present in Fig. 2 (A). We adopt MACE-MP-0¹⁷ as the backbone U-MLIP due to its strong reported performance and scalability, but emphasize that FIRE is conceptually general and applicable to other universal interatomic potentials. Fig. 2 (B,C) show the results of energy and force calculations for different models. The force predictions of the fine-tuned models against DFT calculations (Fig. 2 (B)) present well agreements for all systems, indicating that FIRE preserves quantum-level accuracy even in heterogeneous environments. The accuracy in terms of energy and force RMSEs is measured and shown in Fig. 2 (C). Compared with the from-scratch training, vanilla fine-tuning

(viz. without replay mechanism), and previously reported results, the FIRE achieves the lowest errors, suppressing energy RMSEs to below 1 meV/atom and force RMSEs to 20 meV/Å across diverse solid–solid interfaces. Current MLIPs for battery materials typically report energy errors exceeding 3 meV/atom and force errors surpassing 100 meV/Å (RMSE or MAE).^{44,47,49–54} Hence, FIRE establishes a practical paradigm for constructing significantly more accurate MLIPs. Details about frameworks including loss curves and accuracies reported in the existed works are summarized in Fig. S1 and Table S2 in SI, respectively.

The predictive performance and computational efficiency of FIRE are assessed with the variable size of datasets. Fig. 3 (A,B) presents PCA projections of the sampled configurations for two representative systems: Na/Na₃SbS₄ (top) and Li₇La₃Zr_{2-x}M_xO₁₂ (M = Ta, Nb) (bottom). With the increase of the dataset size from 500 to 4000 frames, the configurational manifolds become increasingly well-resolved, indicating enhanced structural diversity and more comprehensive coverage of the relevant configurational space. This confirms the effectiveness of our sampling protocol. Details of the sampling procedure are provided in Section S.1 in SI. Accuracy and cost results in Fig. 3 (C,D) illustrate that the FIRE yields the lowest RMSEs for both energy and force across all data sizes and significantly outperforms the vanilla fine-tuning, random sampling and from-scratch training. Notably, the approach scales favorably in computational cost, with sampling contributing only a minor overhead relative to fine-tuning. Together, these results highlight how coupling efficient sampling with continual fine-tuning achieves competitive accuracy with substantially reduced data and cost compared to conventional approaches.

We finally evaluate their predictive power for both electrochemical and mechanical properties of the task-specific MLIPs via molecular dynamics simulations. The results are shown in Fig. 4. For three representative systems (T–Na₃SbS₄, Li_{6.5}La₃Zr_{1.5}Ta_{0.5}O₁₂; LLZTO, and Li₆PS₅Cl; LPSCl), the optimized atomic structures are presented in the left panel of Fig. 4 (A), followed by room-temperature MSD curves in the middle panel. Post-processed diffusion coefficients and ionic conductivities exhibit strong agreement with literature values.^{57–60}

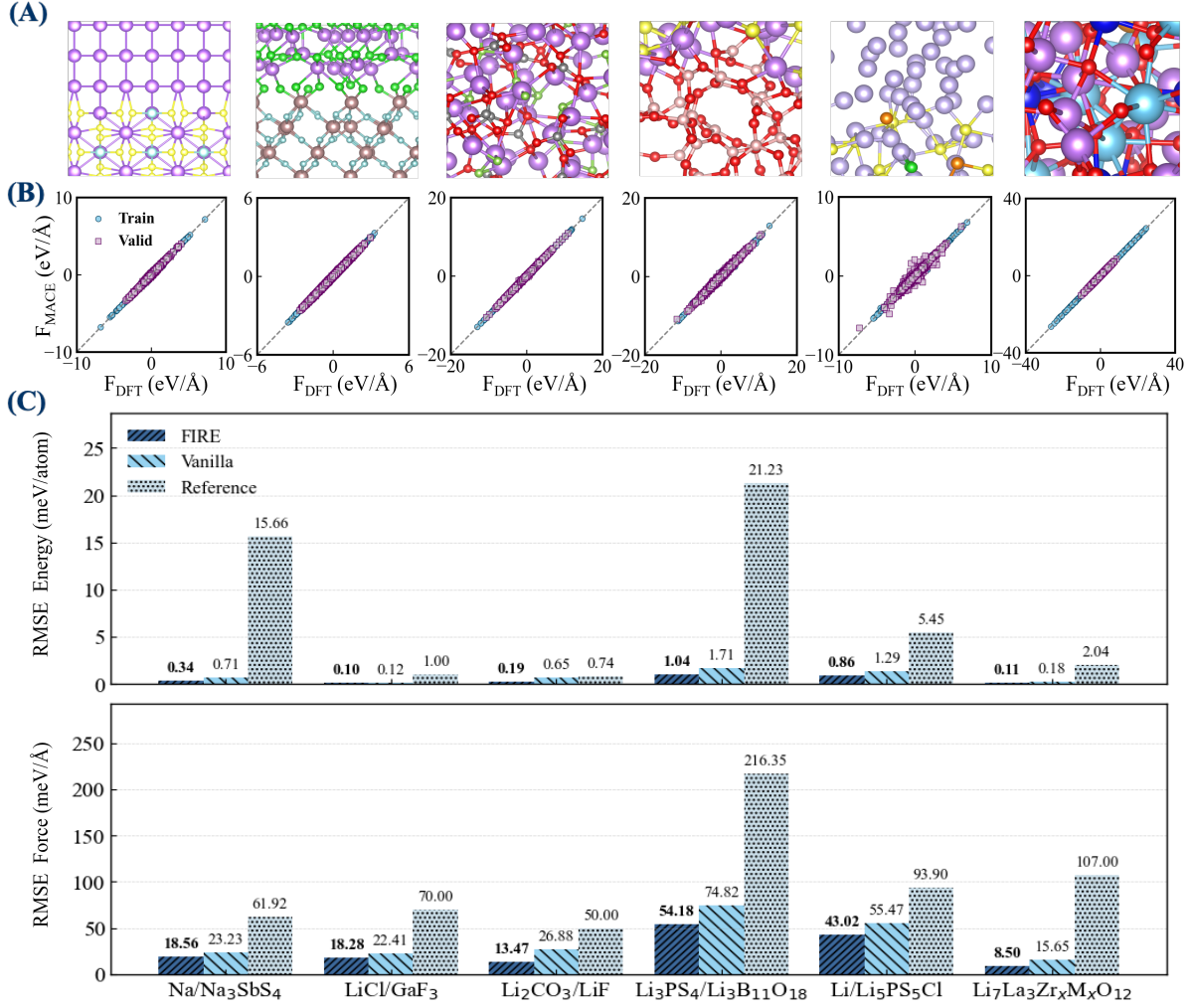


Figure 2: Model evaluation of the FIRE approach: (A) atomic configurations of the six battery materials studied in this work, from left to right: Na/Na₃SbS₄, LiCl/GaF₃, Li₂CO₃/LiF, Li₃PS₄/Li₃B₁₁O₁₈, Li/Li₅PS₅Cl, and Li₇La₃Zr_{2-x}M_xO₁₂ (M = Ta, Nb); (B) the corresponding force predicted by fine-tuned model with respect to that of DFT calculation; (C) model evaluation via RMSE for energy and force, respectively. For comparison, results collected from literature and vanilla fine-tuning are shown.

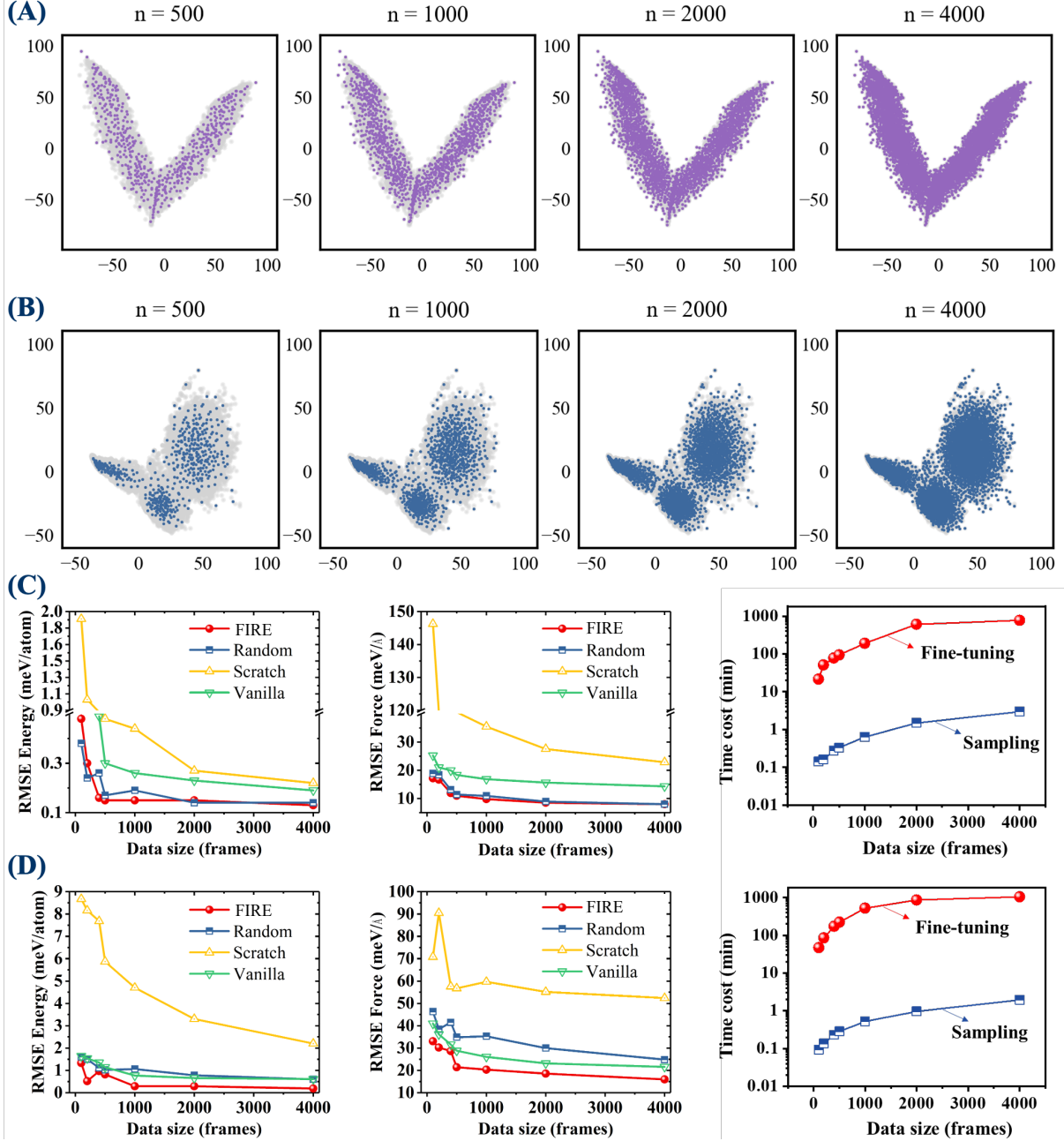


Figure 3: Data efficiency of the FIRE approach: (A–B) PCA projections of sampled configurations for $\text{Na}/\text{Na}_3\text{SbS}_4$ and $\text{Li}_7\text{La}_3\text{Zr}_{2-x}\text{M}_x\text{O}_{12}$ ($M = \text{Ta}, \text{Nb}$), showing broader structural coverage with increasing dataset size; (C–D) data-efficiency benchmarks: replay-argumented fine-tuning achieves the lowest energy and force errors with reduced computational cost, outperforming vanilla fine-tuning, random sampling, and from-scratch training.

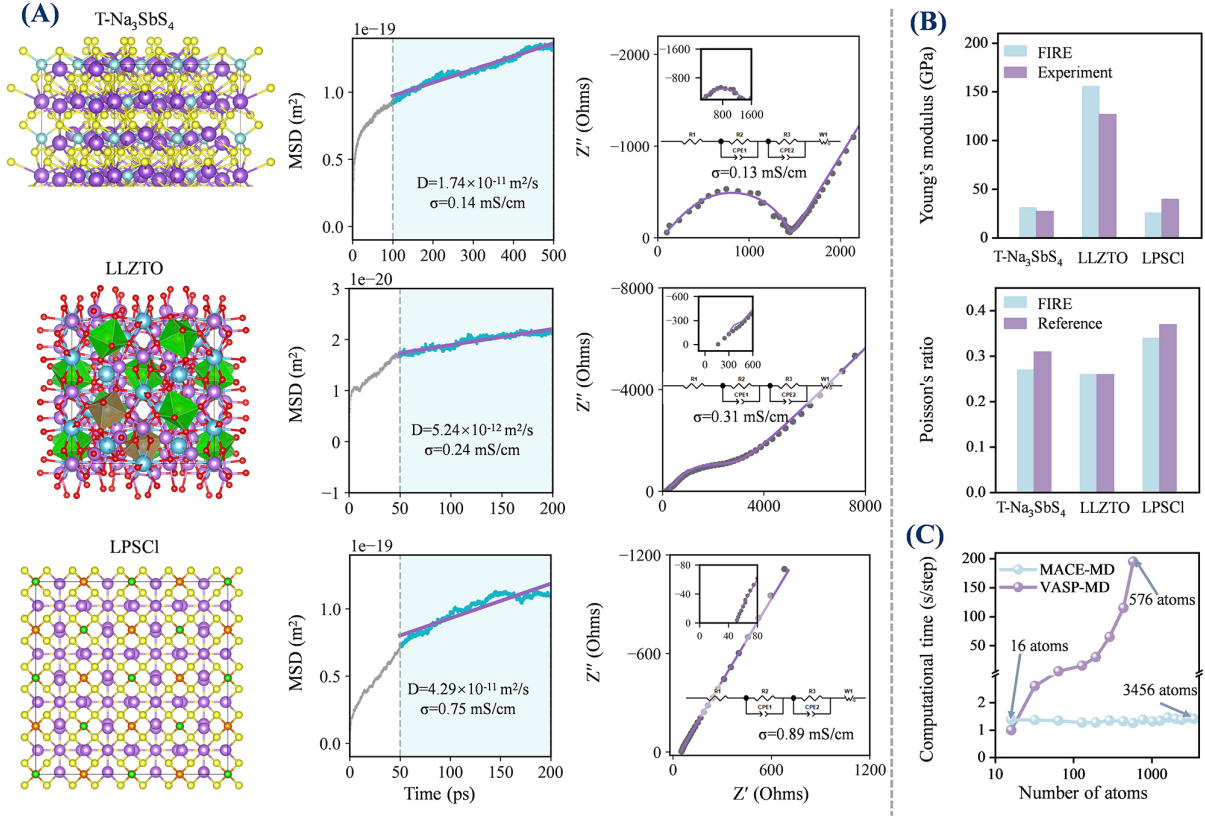


Figure 4: Property predictions from FIRE-generated fine-tuned MLIP models. (A) First column: Optimized structures of T-Na₃SbS₄, LLZTO, and LPSCl. Second column: Mean square displacement (MSD) curves from MACE-MD simulations at relevant temperatures. Third column: Room-temperature impedance spectra with equivalent circuit fits. (B) Comparison of predicted Young's modulus and Poisson's ratio against experimental values. Young's modulus was obtained by spatially averaging AFM nanomechanical maps. Reference values of Poisson's ratios are taken from: T-Na₃SbS₄,⁵⁵ LLZTO,⁵⁶ and LPSCl.³ (C) Scaling of MD wall time per simulation step. MLIP-based MD maintains nearly constant cost up to 3456 atoms, in contrast to the cubic scaling behavior of VASP-based MD.

The right panel shows Nyquist plots from electrochemical impedance spectroscopy, where conductivities from MLIP-MD match experimental measurements⁶¹ closely, highlighting the transferability and reliability of our fine-tuned models trained by the FIRE approach. Based on the Nernst-Einstein relation with a Haven-ratio correction,^{58–60} these findings minimize discrepancies between simulated and measured results. In addition to electrochemical properties (e.g., ionic conductivities), interfacial mechanics play a critical role in battery performance, particularly at solid-solid interfaces. As shown in Fig. 4 (B), by comparing with both experimental measurements (viz. atomic force microscopy shown in Fig. S2 in SI) for Young’s modulus, and first-principle calculations for Poisson’s ratio, the fine-tuned MLIPs capture mechanical response with relatively high accuracy. Finally, computational efficiency is benchmarked in Fig. 4 (C). Dynamical simulations through fine-tuned MLIPs maintain nearly constant wall-time per MD step from 16 to 3456 atoms, whereas first-principles methods exhibit cubic scaling and are practically limited to 600 atoms due to memory bottlenecks. Together, Fig. 4 demonstrates that the fine-tuned models from FIRE not only reproduce transport and mechanical properties in close agreement with experiments, but also extend atomistic simulations to time and length scales inaccessible to ab initio methods. Details about sample preparation and characterization (viz. X-ray diffraction shown in Fig. S3) are given in Section S.4 in SI.

Conclusions

In summary, this work develops FIRE, a data-efficient and accurate framework, for modeling solid–solid interfaces in battery materials through the fine-tuning of U-MLIPs. By coupling targeted data generation with dimensionality reduction and a replay-augmented continual fine-tuning protocol, the FIRE approach achieves state-of-the-art accuracy (energy errors below 1 meV/atom and force errors near 20 meV/Å) while requiring significantly less training data than existing methods. The approach is validated across chemically diverse interfaces

and accurately reproduces key electrochemical and mechanical properties, underscoring its potential for reliable and scalable atomistic modeling of complex battery systems. In future work, uncertainty-aware active learning protocols can be integrated with the FIRE to achieve long-timescale and multiscale simulations, thereby enhancing its generality and accelerating the predictive design of next-generation energy materials.

Acknowledgement

The authors acknowledge the developers of MACE and the MACE GitHub community (<https://github.com/ACEsuit/mace>) for their insightful feedback and implementation support. Their contributions provided the foundation for our proposed FIRE strategy.

Funding

Z. Xu and T. Zhao acknowledge the support from the National Natural Science Foundation of China (NNSFC) (grants No. 12426304 and 12325113), and the Science and Technology Commission of Shanghai Municipality (STCSM) (grant No. 23JC1402300). S.-H. Bo acknowledges the support from NNSFC (grants No. 22222204, 22393902 and 12426304), and the STCSM (grants No. 24DZ3001402 and 23TS1401600). T. Zhao acknowledges the support from the Natural Science Foundation of Chongqing (grant No. CSTB2024NSCQ-MSX1238).

Supporting Information Available

The following files are available free of charge.

- S.1 Details of the FIRE Framework
- S.2 Details on Dataset Generation
- S.3 Details on MD Simulations

- S.4 Details on Experiments

Data availability

Data is provided within the supplementary information file.

Author contributions

X. Liu performed the calculations including the generation of the dataset and drafted the manuscript. X. Yu contributed to the experiments including sample preparation and characterization. Y. Wang developed the framework proposed in this work, finalized the workflow with optimized settings, and wrote the manuscript. Z.-T. Sun prepared dataset of LLZTO and analyzed the results. Z. Luo conducted the MD simulations and analysis. K. Zeng performed model training and validation. T. Zhao designed the workflow of this work and polished the language. S.-H. Bo and Z. Xu supervised the research. All authors contributed to the discussions and provided feedback on the manuscript.

Correspondence and requests for materials should be addressed to T. Zhao or S.-H. Bo or Z. Xu.

Competing interests

All authors declare no financial or non-financial competing interests.

References

- (1) Xu, L.; Tang, S.; Cheng, Y.; Wang, K.; Liang, J.; Liu, C.; Cao, Y.-C.; Wei, F.; Mai, L. Interfaces in solid-state lithium batteries. *Joule* **2018**, *2*, 1991–2015.

(2) Sun, Z.-T.; Chen, S.; Zhao, T.; Guo, Y.; Xu, Z.; Zhou, S.; Bo, S.-H. Real 2D Galvanostatic Model: Encoding Physicochemical Heterogeneity into a Full Battery. *Physical Review Letters* **2025**, *135*, 068001.

(3) Chen, S.; Cao, Q.; Tang, B.; Yu, X.; Zhou, Z.; Bo, S.-H.; Guo, Y. Chemomechanical pairing of alloy anodes and Solid-State electrolytes. *ACS Energy Letters* **2024**, *9*, 5373–5382.

(4) Sun, Z.-T.; Zhou, J.; Wu, Y.; Bo, S.-H. Mapping and modeling physicochemical fields in solid-state batteries. *The Journal of Physical Chemistry Letters* **2022**, *13*, 10816–10822.

(5) Behler, J.; Parrinello, M. Generalized neural-network representation of high-dimensional potential-energy surfaces. *Physical Review Letters* **2007**, *98*, 146401.

(6) Zhang, L.; Han, J.; Wang, H.; Car, R.; E, W. Deep potential molecular dynamics: A scalable model with the accuracy of quantum mechanics. *Physical Review Letters* **2018**, *120*, 143001.

(7) Deringer, V. L. Modelling and understanding battery materials with machine-learning-driven atomistic simulations. *Journal of Physics: Energy* **2020**, *2*, 041003.

(8) Euchner, H.; Groß, A. Atomistic modeling of Li-and post-Li-ion batteries. *Physical Review Materials* **2022**, *6*, 040302.

(9) Olsson, E.; Yu, J.; Zhang, H.; Cheng, H.-M.; Cai, Q. Atomic-scale design of anode materials for alkali metal (Li/Na/K)-ion batteries: Progress and perspectives. *Advanced Energy Materials* **2022**, *12*, 2200662.

(10) Bartók, A. P.; Payne, M. C.; Kondor, R.; Csányi, G. Gaussian approximation potentials: The accuracy of quantum mechanics, without the electrons. *Physical Review Letters* **2010**, *104*, 136403.

(11) Drautz, R. Atomic cluster expansion for accurate and transferable interatomic potentials. *Physical Review B* **2019**, *99*, 014104.

(12) Schütt, K. T.; Sauceda, H. E.; Kindermans, P.-J.; Tkatchenko, A.; Müller, K.-R. SchNet – A deep learning architecture for molecules and materials. *The Journal of Chemical Physics* **2018**, *148*, 241722.

(13) Batatia, I.; Kovacs, D. P.; Simm, G.; Ortner, C.; Csányi, G. MACE: Higher order equivariant message passing neural networks for fast and accurate force fields. *Advances in Neural Information Processing Systems* **2022**, *35*, 11423–11436.

(14) Cheng, B. Cartesian atomic cluster expansion for machine learning interatomic potentials. *npj Computational Materials* **2024**, *10*, 157.

(15) Ji, Y.; Liang, J.; Xu, Z. Machine-learning interatomic potentials for long-range systems. arXiv:2502.04668, 2025.

(16) Jain, A.; Ong, S. P.; Hautier, G.; Chen, W.; Richards, W. D.; Dacek, S.; Cholia, S.; Gunter, D.; Skinner, D.; Ceder, G.; Persson, K. A. Commentary: The Materials Project: A materials genome approach to accelerating materials innovation. *APL Materials* **2013**, *1*, 011002.

(17) Batatia, I.; Benner, P.; Chiang, Y.; Elena, A. M.; Kovács, D. P.; Riebesell, J.; Advincula, X. R.; Asta, M.; Avaylon, M.; Baldwin, W. J.; et al. A foundation model for atomistic materials chemistry. arXiv:2401.00096, 2023.

(18) Deng, B.; Zhong, P.; Jun, K.; Riebesell, J.; Han, K.; Bartel, C. J.; Ceder, G. CHGNet as a pretrained universal neural network potential for charge-informed atomistic modelling. *Nature Machine Intelligence* **2023**, *5*, 1031–1041.

(19) Liao, Y.-L.; Wood, B.; Das, A.; Smidt, T. EquiformerV2: Improved equivariant transformer for scaling to higher-degree representations. arXiv:2306.12059, 2023.

(20) Yang, H.; Hu, C.; Zhou, Y.; Liu, X.; Shi, Y.; Li, J.; Li, G.; Chen, Z.; Chen, S.; Zeni, C.; et al. Mattersim: A deep learning atomistic model across elements, temperatures and pressures. arXiv:2405.04967, 2024.

(21) Zhang, D.; Bi, H.; Dai, F.-Z.; Jiang, W.; Liu, X.; Zhang, L.; Wang, H. Pretraining of attention-based deep learning potential model for molecular simulation. *npj Computational Materials* **2024**, *10*, 94.

(22) Neumann, M.; Gin, J.; Rhodes, B.; Bennett, S.; Li, Z.; Choubisa, H.; Hussey, A.; Godwin, J. Orb: A fast, scalable neural network potential. arXiv:2410.22570, 2024.

(23) Xie, F.; Lu, T.; Meng, S.; Liu, M. GPTFF: A high-accuracy out-of-the-box universal AI force field for arbitrary inorganic materials. *Science Bulletin* **2024**, *69*, 3525–3532.

(24) Park, Y.; Kim, J.; Hwang, S.; Han, S. Scalable parallel algorithm for graph neural network interatomic potentials in molecular dynamics simulations. *Journal of Chemical Theory and Computation* **2024**, *20*, 4857–4868.

(25) Merchant, A.; Batzner, S.; Schoenholz, S. S.; Aykol, M.; Cheon, G.; Cubuk, E. D. Scaling deep learning for materials discovery. *Nature* **2023**, *624*, 80–85.

(26) Nomura, K.-i.; Hattori, S.; Ohmura, S.; Kanemasu, I.; Shimamura, K.; Dasgupta, N.; Nakano, A.; Kalia, R. K.; Vashishta, P. Allegro-FM: Toward an Equivariant Foundation Model for Exascale Molecular Dynamics Simulations. *The Journal of Physical Chemistry Letters* **2025**, *16*, 6637–6644.

(27) Kim, K.; Adelstein, N.; Dive, A.; Grieder, A.; Kang, S.; Wood, B. C.; Wan, L. F. Probing degradation at solid-state battery interfaces using machine-learning interatomic potential. *Energy Storage Materials* **2024**, *73*, 103842.

(28) Staacke, C. G.; Heenen, H. H.; Scheurer, C.; Csányi, G.; Reuter, K.; Margraf, J. T.

On the role of long-range electrostatics in machine-learned interatomic potentials for complex battery materials. *ACS Applied Energy Materials* **2021**, *4*, 12562–12569.

(29) Ju, S.; You, J.; Kim, G.; Park, Y.; An, H.; Han, S. Application of pretrained universal machine-learning interatomic potential for physicochemical simulation of liquid electrolytes in Li-ion batteries. *Digital Discovery* **2025**, *4*, 1544–1559.

(30) Kim, K.; Dive, A.; Grieder, A.; Adelstein, N.; Kang, S.; Wan, L. F.; Wood, B. C. Flexible machine-learning interatomic potential for simulating structural disordering behavior of $\text{Li}_7\text{La}_3\text{Zr}_2\text{O}_{12}$ solid electrolytes. *The Journal of Chemical Physics* **2022**, *156*, 221101.

(31) Hajibabaei, A.; Kim, K. S. Universal machine learning interatomic potentials: surveying solid electrolytes. *The Journal of Physical Chemistry Letters* **2021**, *12*, 8115–8120.

(32) Wang, F.; Ma, Z.; Cheng, J. Accelerating computation of acidity constants and redox potentials for aqueous organic redox flow batteries by machine learning potential-based molecular dynamics. *Journal of the American Chemical Society* **2024**, *146*, 14566–14575.

(33) Diddens, D.; Appiah, W. A.; Mabrouk, Y.; Heuer, A.; Vegge, T.; Bhowmik, A. Modeling the solid electrolyte interphase: Machine learning as a game changer? *Advanced Materials Interfaces* **2022**, *9*, 2101734.

(34) Wang, J.; Panchal, A. A.; Canepa, P. Strategies for fitting accurate machine-learned inter-atomic potentials for solid electrolytes. *Materials Futures* **2023**, *2*, 015101.

(35) Zheng, Z.; Zhou, J.; Zhu, Y. Computational approach inspired advancements of solid-state electrolytes for lithium secondary batteries: from first-principles to machine learning. *Chemical Society Reviews* **2024**, *53*, 3134–3166.

(36) Maevskiy, A.; Carvalho, A.; Sataev, E.; Turchyna, V.; Noori, K.; Rodin, A.; Castro Neto, A.; Ustyuzhanin, A. Predicting ionic conductivity in solids from the machine-learned potential energy landscape. *Physical Review Research* **2025**, *7*, 023167.

(37) Zhong, P.; Kim, D.; King, D. S.; Cheng, B. Machine learning interatomic potential can infer electrical response. arXiv:2504.05169, 2025.

(38) Li, H.; Zhu, C.; Zhang, Y.; Sun, Y.; Shui, Z.; Kuang, W.; Zheng, S.; Yang, L. Task-specific fine-tuning via variational information bottleneck for weakly-supervised pathology whole slide image classification. IEEE Conference on Computer Vision and Pattern Recognition. 2023; pp 7454–7463.

(39) Kaur, H.; Della Pia, F.; Batatia, I.; Advincula, X. R.; Shi, B. X.; Lan, J.; Csányi, G.; Michaelides, A.; Kapil, V. Data-efficient fine-tuning of foundational models for first-principles quality sublimation enthalpies. *Faraday Discussions* **2025**, *256*, 120–138.

(40) Bartók, A. P.; Kondor, R.; Csányi, G. On representing chemical environments. *Physical Review B* **2013**, *87*, 184115.

(41) Himanen, L.; Jánka, P.; Morooka, E. V.; Canova, F. F.; Ranawat, Y. S.; Zouboulis, K.; Gazda, L.; Foster, A. S. Dscribe: Library of descriptors for machine learning in materials science. *Communications in Computational Physics* **2020**, *247*, 106949.

(42) Feng, S.; Cai, A.; Wang, Y.; Zhang, B.; Qiao, Q.; Chen, C.; Wang, S.; Jiang, J. A robotic AI-Chemist system for multi-modal AI-ready database. *National Science Review* **2023**, *10*, 332.

(43) An, Y.; Hu, T.; Pang, Q.; Xu, S. Observing Li Nucleation at the Li Metal–Solid Electrolyte Interface in All-Solid-State Batteries. *ACS Nano* **2025**, *19*, 14262–14271.

(44) Lee, J.; Ju, S.; Hwang, S.; You, J.; Jung, J.; Kang, Y.; Han, S. Disorder-dependent Li

diffusion in $\text{Li}_6\text{PS}_5\text{Cl}$ investigated by machine-learning potential. *ACS Applied Materials & Interfaces* **2024**, *16*, 46442–46453.

(45) Wang, C.; Aykol, M.; Mueller, T. Nature of the amorphous–amorphous interfaces in solid-state batteries revealed using machine-learned interatomic potentials. *Chemistry of Materials* **2023**, *35*, 6346–6356.

(46) Hu, T.; Tian, J.; Dai, F.; Wang, X.; Wen, R.; Xu, S. Impact of the local environment on Li ion transport in inorganic components of solid electrolyte interphases. *Journal of the American Chemical Society* **2022**, *145*, 1327–1333.

(47) You, Y.; Zhang, D.; Wu, F.; Cao, X.; Sun, Y.; Zhu, Z.-Z.; Wu, S. Principal component analysis enables the design of deep-learning potential precisely capturing LLZO phase transitions. *npj Computational Materials* **2024**, *10*, 57.

(48) Kim, D.; King, D. S.; Zhong, P.; Cheng, B. Learning charges and long-range interactions from energies and forces. arXiv:2412.15455, 2024.

(49) Ren, F.; Wu, Y.; Zuo, W.; Zhao, W.; Pan, S.; Lin, H.; Yu, H.; Lin, J.; Lin, M.; Yao, X.; Brezesinski, T.; Gong, Z.; Yang, Y. Visualizing the SEI formation between lithium metal and solid-state electrolyte. *Energy & Environmental Science* **2024**, *17*, 2743–2752.

(50) Ou, Y.; Ikeda, Y.; Scholz, L.; Divinski, S.; Fritzen, F.; Grabowski, B. Atomistic modeling of bulk and grain boundary diffusion in solid electrolyte $\text{Li}_6\text{PS}_5\text{Cl}$ using machine-learning interatomic potentials. *Physical Review Materials* **2024**, *8*, 115407.

(51) Lai, G.; Zuo, Y.; Fang, C.; Huang, Z.; Chen, T.; Liu, Q.; Cui, S.; Zheng, J. Unraveling charge effects on interface reactions and dendrite growth in lithium metal anode. *npj Computational Materials* **2025**, *11*, 121.

(52) Holekevi Chandrappa, M. L.; Qi, J.; Chen, C.; Banerjee, S.; Ong, S. P. Thermodynamics and kinetics of the cathode–electrolyte interface in all-solid-state Li–S batteries. *Journal of the American Chemical Society* **2022**, *144*, 18127–18139.

(53) Li, B. Y.; Karan, V.; Kaplan, A. D.; Wen, M.; Persson, K. A. An atomistic study of reactivity in solid-state electrolyte interphase formation for Li/Li₇P₃S₁₁. *The Journal of Physical Chemistry C* **2025**, *129*, 16043–16054.

(54) Jang, M.; Park, K.; Lee, Y.; Shim, J. H.; Kim, K.; Yu, S. Mechanistic insights into superionic thioarsenate argyrodite solid electrolytes via machine learning interatomic potentials. *Journal of Materials Chemistry A* **2025**, 10.1039/D5TA05538E.

(55) Awais, M.; Dorigo, T.; Sandin, F.; Coradin, E.; Nguyen, X.-T.; Lupi, E.; De Vita, A. Computational Evaluation of Na₃SbX₃ (X = S, Se) for resistive switching memory devices for Neuromorphic Computing applications. Poster, 2024; Poster presented at the 4th MODE Workshop on Differentiable Programming for Experiment Design (MODE 2024), Valencia, Spain, Sep 23–25, 2024.

(56) Yu, S.; Schmidt, R. D.; Garcia-Mendez, R.; Herbert, E.; Dudney, N. J.; Wolfenstein, J. B.; Sakamoto, J.; Siegel, D. J. Elastic properties of the solid electrolyte Li₇La₃Zr₂O₁₂ (LLZO). *Chemistry of Materials* **2016**, *28*, 197–206.

(57) Sau, K.; Takagi, S.; Ikeshoji, T.; Kisu, K.; Sato, R.; Dos Santos, E. C.; Li, H.; Mohtadi, R.; Orimo, S.-i. Unlocking the secrets of ideal fast ion conductors for all-solid-state batteries. *Communications Materials* **2024**, *5*, 122.

(58) Klarbring, J.; Walsh, A. Na vacancy-driven phase transformation and fast ion conduction in W-doped Na₃SbS₄ from machine learning force fields. *Chemistry of Materials* **2024**, *36*, 9406–9413.

(59) Dorai, A.; Kuwata, N.; Takekawa, R.; Kawamura, J.; Kataoka, K.; Akimoto, J. Diffusion

coefficient of lithium ions in garnet-type $\text{Li}_{6.5}\text{La}_3\text{Zr}_{1.5}\text{Ta}_{0.5}\text{O}_{12}$ single crystal probed by ^{7}Li pulsed field gradient-NMR spectroscopy. *Solid State Ionics* **2018**, *327*, 18–26.

(60) Adeli, P.; Bazak, J. D.; Park, K. H.; Kochetkov, I.; Huq, A.; Goward, G. R.; Nazar, L. F. Boosting solid-state diffusivity and conductivity in lithium superionic argyrodites by halide substitution. *Angewandte Chemie International Edition* **2019**, *58*, 8681–8686.

(61) Tang, B.; Zhao, Y.; Wang, Z.; Chen, S.; Wu, Y.; Tseng, Y.; Li, L.; Guo, Y.; Zhou, Z.; Bo, S.-H. Ultrathin salt-free polymer-in-ceramic electrolyte for solid-state sodium batteries. *eScience* **2021**, *1*, 194–202.